Molecular Crystals and Liquid Crystals
Publication details, including instructions for authors and subscription information:
http://www.tandfonline.com/loi/gmcl20

Conductivity Mechanisms in a Composite of Chitosan-Silver Nanoparticles

E. Prokhorov [a], J. G. Luna-Bárcenas [a], J. B. González-Campos [b] & I. C. Sanchez [c]

[a] Cinvestav Unidad Querétaro, Querétaro, Qro., México

[b] Universidad Michoacana de San Nicolás de Hidalgo, Morelia, Michoacán, México

[c] Department of Chemical Engineering, The University of Texas at Austin, Austin, TX, USA

Version of record first published: 03 Mar 2011

To cite this article: E. Prokhorov, J. G. Luna-Bárcenas, J. B. González-Campos & I. C. Sanchez (2011): Conductivity Mechanisms in a Composite of Chitosan-Silver Nanoparticles, Molecular Crystals and Liquid Crystals, 536:1, 24/[256]-32/[264]

To link to this article: http://dx.doi.org/10.1080/15421406.2011.538327

Mol. Cryst. Liq. Cryst., Vol. 536: pp. 24/[256]–32/[264], 2011

ISSN: 1542-1406 print/1563-5287 online
DOI: 10.1080/15421406.2011.538327

Conductivity Mechanisms in a Composite of Chitosan-Silver Nanoparticles

E. PROKHOROV,[1] J. G. LUNA-BÁRCENAS,[1]
J. B. GONZÁLEZ-CAMPOS,[2] AND I. C. SANCHEZ[3]

[1]Cinvestav Unidad Querétaro, Querétaro, Qro., México
[2]Universidad Michoacana de San Nicolás de Hidalgo, Morelia, Michoacán, México
[3]Department of Chemical Engineering, The University of Texas at Austin, Austin, TX, USA

The aim of this work was to investigate the conductivity mechanisms of a bionanocomposite of chitosan-silver nanoparticles. The DC conductivity in dry samples shows that the composite exhibits a percolation threshold at about 2% volume fraction of nanoparticles. For films with less than 2%, the temperature dependence of the DC conductivity in the range 2–70° C exhibits the two-dimensional hopping conductivity. For all nanocomposites in the temperature range 70–180° C, both conductivity and relaxation times obtained from electrical module measurements demonstrate an Arrhenius-type temperature dependence. This behavior is associated with the migration property of movable hydrogen ions and the formation of dipolar structures.

Keywords Bionanocomposites; chitosan; conductivity; silver nanoparticles

1. Introduction

Chitosan (CS), a natural polysaccharide derived from naturally occurring chitin, possesses a striking combination of properties such as biocompatibility, biodegradability, and non-toxicity. Its antibacterial activity makes it an exceptional material for biomedical applications. Additionally, chitosan is soluble in aqueous acidic media. The proper combination of such properties allows for the formation of bionanocomposites of chitosan-metal nanoparticles. Among chitosan-based nanocomposites, chitosan/silver nanoparticles (Ag*nP*'s) is an attractive biomaterial because of its great potential in biomedicine including its antimicrobial activity [1]. Other applications include biosensors and electrolytes for fuel cells [1–3]. For the latter application, the conductivity mechanism of CS/Ag*nP*'s nanocomposites has not been previously addressed. In the literature, most publications focus on the fabrication, microstructural characterization, and antibacterial activity of the nanocomposites [1,2,4], but not on the conductivity mechanisms.

Address correspondence to E. Prokhorov, Cinvestav Unidad Querétaro, Querétaro, Qro., 76230, México. E-mail: prokhorov@qro.cinvestav.mx

Pristine dry chitosan exhibits ionic conductivities between 10^{-9}–10^{-11} S cm^{-1} [3,5] mainly due to its free amino groups. The absorption of ambient water leads to the protonation of the amine groups by increasing the conductivity to 10^{-4} S cm^{-1} [3]. The water absorption in pure chitosan is responsible for the appearance of the low-frequency α-relaxation associated with the glass-rubber transition [5]. In contrast, dry chitosan exhibits no glass transition. Similar moisture effects on the molecular dynamics and the conductivity have been observed in CS/Ag*nP*'s nanocomposites [6]. The aim of this work is to synthesize CS/Ag*nP*'s composites and to investigate the influence of silver nanoparticles on the conductivity mechanisms of dry bionanocomposites.

2. Materials and Methods

CS/Ag*nP*'s films were obtained by dissolving chitosan (82% of degree of deacetylation) and a powder of silver nanoparticles (25-nm average particle size, and the contents of nanoparticles are between 0–20 wt.%) in a 1 wt.% aqueous acetic acid solution with subsequent stirring to promote the dissolution and the elimination of a bubble formation. CS/Ag*nP*'s films (with thickness of about 30 μm) were prepared by the solvent cast method by pouring the final solution into a plastic Petri dish and allowing the solvent to evaporate for 24 h at 60°C. Because of the films preparation technique, the chitosan films exhibit the ionic conductivity due to the presence of protonated amino side group (NH_3^+). SEM micrographs show a homogeneous distribution of silver nanoparticles and agglomerates with an average dimension of 200 nm [6]. The Fourier Transformed Infrared spectroscopy analysis reveals the interaction of silver nanoparticles with OH, NH_2, $CO \cdot NH_2$, and C-O-C groups implying an evident redistribution of the vibration bands for these groups [6].

Dielectric temperature measurements from 2 to 250°C in the frequency range from 100 Hz to 110 MHz were carried out using an Agilent Precision Impedance Analyzer 4294A in a vacuum cell on films with two gold contacts. Before measurements, all films were annealed in the impedance cell at 120°C under vacuum for 1 h followed by the cooling to 2°C to ensure the entire water removal.

3. Results

Figure 1 shows the plots of the DC electrical conductivity obtained from the fitting procedure described above as a function of the Ag*nP*'s volume fraction at room temperature. An abrupt increase of the conductivity with increasing f and a subsequent saturation is typically observed for percolation phenomena. Such a behavior of the DC conductivity in percolation systems has been reported in various types of disordered polymer-conductor composites [7,8]. According to percolation theory, the DC conductivity in a vicinity of the percolation threshold can be characterized by the simple power law [9]:

$$\sigma \propto (f - f_c)^t, \tag{1}$$

where f is the volume fraction of the conductivity phase, f_c is the critical volume fraction at the percolation threshold, and t is the critical exponent which is only

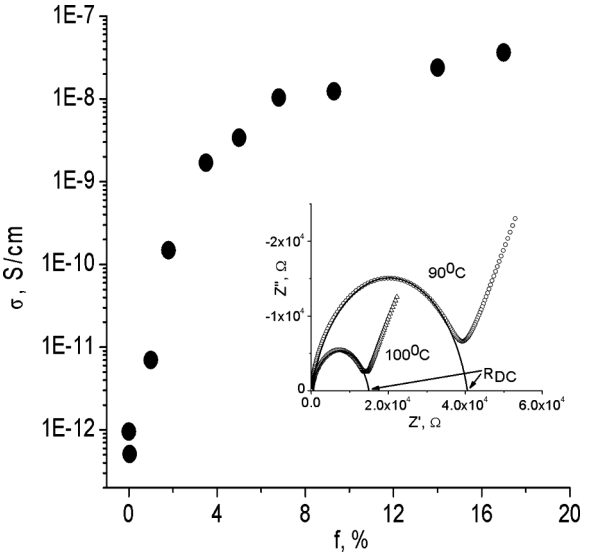

Figure 1. The electrical conductivity of CS/Ag*nP*'s films as a function of the Ag*nP*'s volume fraction. The insert shows the complex impedance spectra obtained in a film with 10 wt.% of Ag*nP*'s at the temperature indicated on the graph.

dependent on the dimensionality of the percolation system with values typically around 1.3 and 2.0 for two and three-dimensions, respectively [10]. On the other hand, the static dielectric constant ε of a percolating system exhibits the following power-law dependence below of the percolation threshold [11]:

$$\varepsilon \propto (f_c - f)^{-s}. \tag{2}$$

The insert in Figure 1 shows the typical complex impedance spectra measured in all films. This plot exhibits the characteristic depressed semicircles at high frequencies and the quasilinear response at low frequencies. According to the previously reported studies [3,6], a depressed semicircle describes properties of a bulk material, and the quasilinear response at low frequencies is associated with the interfacial polarization and/or the surface and contact effects. The values of DC resistance R_{dc} and the corresponding DC conductivity σ_{dc} ($\sigma_{\mathrm{dc}} = d/R_{\mathrm{dc}} \cdot S$, where d is the film thickness, and S is the contact area) have been obtained from the intersection of the high frequency semicircle and the real axis on the impedance plane, as is shown in the insert in Figure 1. The static dielectric constant has been estimated from fitting the same high-frequency semicircle using the ZView program®.

The volume fraction of Ag*nP*'s f in the insulator chitosan matrix has been calculated by using the relation [10]

$$f = \frac{m/V - \rho_{Ag}}{\rho_{CS} - \rho_{Ag}}, \tag{3}$$

where m is the film mass, V is the film volume, ρ_{Ag} is the Ag density, and ρ_{CS} is the chitosan density, respectively.

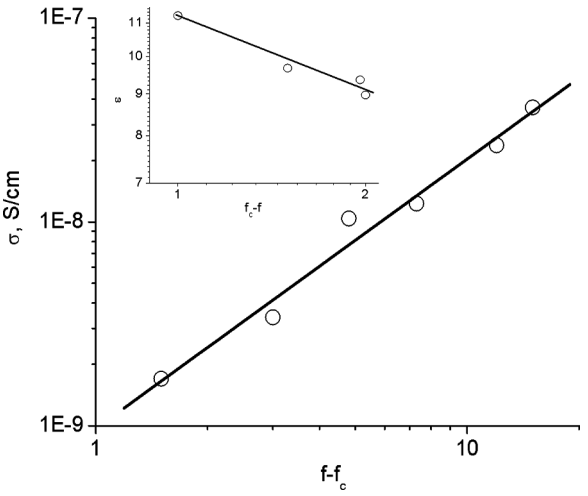

Figure 2. A double log-log plot of the electrical conductivity of the CS/Ag*nP's* composites vs $f-f_c$. The solid line is the best fit according to relation (2). Insert shows the log-log plot of the static dielectric constant ε vs f_c-f (solid line is the fitting by relation (3)).

Figure 2 represents the best fit of the experimental data presented in Figure 1 as a function of $f-f_c$ according to relation (2). This analysis gives the percolation threshold of ca. 2% of the Ag*nP*'s volume fraction and the critical exponent t of 1.32 ± 0.09 which implies that the CS/Ag*nP*'s system is two-dimensional according to the well-established values [10]. The insert in Figure 2 shows the log-log dependence of the static dielectric constant of the CS/Ag*nP*'s composites on $f_c - f$.

The frequency dependence of the ac conductivity at a constant temperature is well described by the Jonscher power relation [1] $\sigma(w) = \sigma_{dc} + \sigma_{ac} = \sigma_{dc} + Aw^x$, where σ_{dc} and σ_{ac} are the dc and ac conductivities, respectively, w is the angular frequency, A is a constant, and x is an exponent dependent on both the frequency and the temperature at $0 < \mathrm{x} < 1$.

Figure 3 shows the real part of the conductivity as a function of the frequency, and the insert in Figure 3 shows the real part of the complex permittivity measured for the nanocomposites indicated in graphs at 25°C. The value of σ_{dc} can be estimated from the plateau in the frequency dependence of the conductivity, beyond which a power law is valid. Near the percolation threshold, both the ac conductivity $\sigma(w, f)$ and the real part of the permittivity $\varepsilon(w, f)$ show the power-law behavior [11]: $\sigma(w, f) \propto w^x$ and $\varepsilon(w, f) \propto w^{-y}$, where the exponents x and y satisfy the relation: $x + y = 1$. As is seen from Figure 3, the ac conductivity increases linearly with the frequency for the nanocomposites with Ag*nP*'s volume fraction less than 2% with a slope of 0.88 ± 0.04. The real part of the complex permittivity decreases with increase in the frequency at the exponent $y = 0.08 \pm 0.01$ which satisfies the relation $x + y = 1$.

Figure 4 shows the natural logarithm of the dc conductivity *versus* the reciprocal temperature in films with Ag*nP*'s volume fractions of 1 and 5% (before and after the percolation threshold). The dc conductivity of a composite with 5% of Ag*nP*'s exhibits a linear Arrhenius-type dependence which is typical of the percolation systems [12] with an activation energy of 82–88 kJ/mol for composites with different Ag*nP*'s

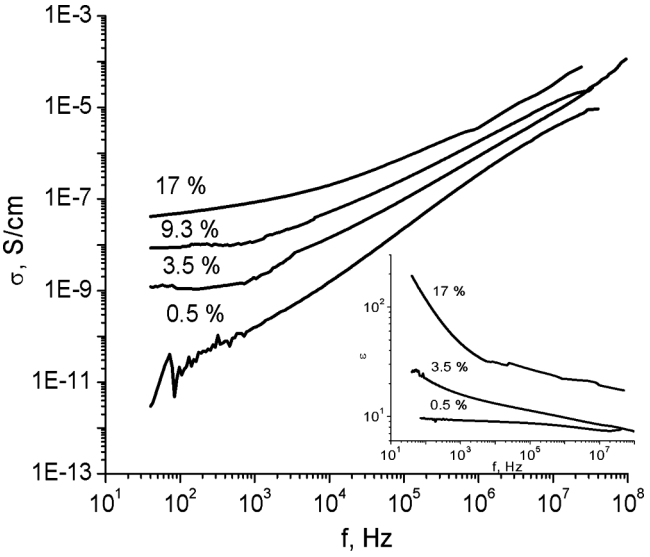

Figure 3. The ac conductivity and the dielectric constant (insert) vs. the frequency for CS/Ag*nP*'s for the volume fraction of Ag*nP*'s indicated on the graph.

volume fractions. The negative slope of the conductivity *versus* the reciprocal temperature can be related to the beginning of degradation processes in the films [6]. In contrast, the films with an Ag*nP*'s volume fraction less than the critical value, the dc conductivity demonstrates a non-linear dependence in the temperature interval 2–70°C and an Arrhenius-type dependence in the range 70–180°C with an activation energy of 87.5 kJ/mol.

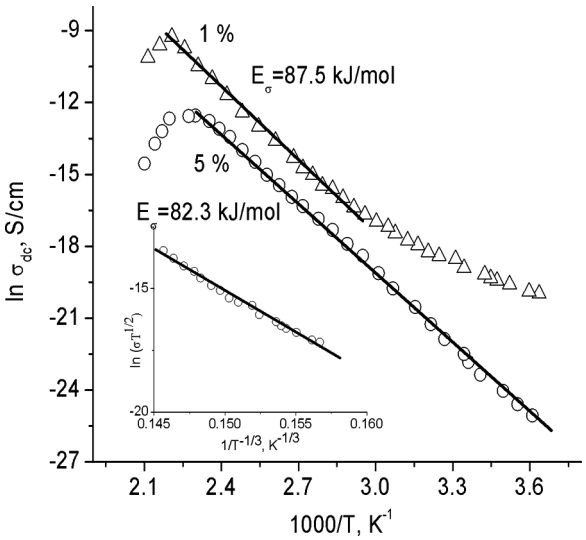

Figure 4. Natural logarithm of the dc conductivity vs the reciprocal temperature in films with Ag*nP*'s volume fractions equal to 1 and 5%. The insert shows $\ln(\sigma T)^{1/2}$ vs $T^{-1/3}$.

Below the percolation threshold, where contacts between metallic inclusions are absent, the dependence of the dc conductivity on the temperature T is often represented by the variable range hopping (VRH) model proposed by Mott [13,14]:

$$\sigma_{dc}(T) = \sigma_0 \exp\left[-\left(\frac{T_0}{T}\right)^{\gamma}\right], \tag{4}$$

where σ_0 can be considered as a limiting conductivity at the infinite temperature, $\sigma_0 \sim 1/T$ [12], T_0 depends on the localization and the density of the states and the exponent γ is related to the dimensionality d of the transport process via the equation $\gamma = 1/(1+d)$, where $d = 1, 2, 3$. The applicability of the VRH model is examined by plotting the experimental results in the form of $\ln(\sigma T)^{1/2}$ vs $T^{-\gamma}$ [14].

Experimental data in the temperature range 2–70°C plotted according to the VRH model are presented in the insert in Figure 4. It is worth noting that the dependence $\ln(\sigma T)^{1/2}$ vs $T^{-\gamma}$ can be linearly fitted with both $\gamma = 1/4$ and $1/3$. However, the best least-square fitting is obtained for $\gamma = 1/3$ (with $R^2 = 0.99$). This value corresponds to the two-dimensional transport process, as explained before.

The calculations of the activation energy in the temperature range 70–180°C give 87 kJ/mol, which is in agreement to the results previously reported for neat chitosan [5].

Dielectric relaxation measurements can give additional information on the conductivity mechanism of nanocomposites. Generally in composites with conductive inclusions and ionic current, the ionic conductivity often masks the real dielectric relaxation processes. To analyze the dielectric process in detail, the complex permittivity ε^* is converted to the complex-valued electric modulus M^* by the following equation:

$$M^* = \frac{1}{\varepsilon^*} = M' + iM'' = \frac{\varepsilon'}{\varepsilon'^2 + \varepsilon''^2} + i\frac{\varepsilon''}{\varepsilon'^2 + \varepsilon''^2}, \tag{5}$$

where M' and M'' are, respectively, the real and imaginary parts of the electric modulus, and ε' and ε'' are, respectively, the real and imaginary parts of the permittivity. Interpreting data in this representation is a commonly employed method to obtain information about the relaxation processes in ionic conductive materials and polymer-metal composites [15,16]. The peak in the imaginary part M'' depends on the temperature, which can be related to the translational ionic motions. The corresponding relaxation time $\tau_\sigma = 1/(2\pi\nu_p)$, where ν_p is the peak frequency, is called the conductivity relaxation time [15].

The imaginary part of the electric modulus *versus* the frequency is shown in Figure 5 for CS/Ag*nP*'s films with Ag*nP*'s volume fraction of 5% at the temperatures indicated on graphs. It can be seen that the increasing temperature shifts the peaks to higher frequencies. The insert shows the Arrhenius plot of the relaxation time calculated from the locations of peaks. The activation energies of 84.5 kJ/mol and 86.9 kJ/mol were obtained for films with Ag*nP*'s volume fractions of 1% and 5%. It is important to note that these values of activation energy correlate well with the activation energies calculated from dc conductivity measurements (Fig. 4) and obtained from the fitting of the complex permittivity in the same composite using the Havriliak–Negami model [6].

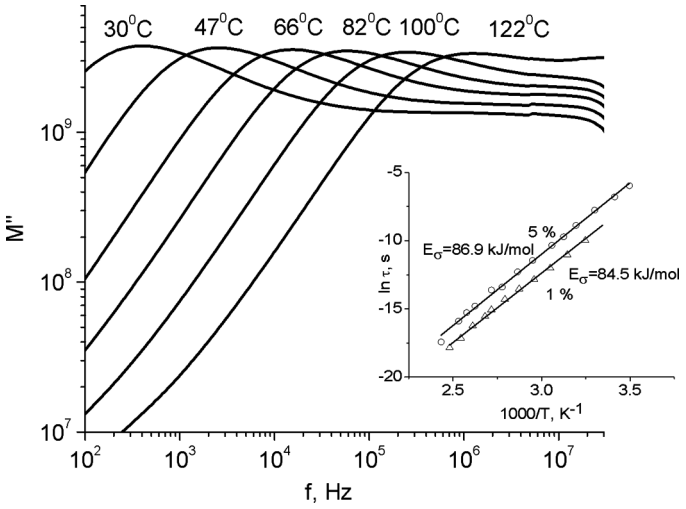

Figure 5. Dependences of the imaginary part of the electric modulus versus the frequency for CS/Ag*nP*'s films with Ag*nP*'s volume fraction of 5% at the temperature indicated on the graphs. Insert shows the Arrhenius plot of the relaxation time calculated from the location of peaks for 1% and 5% of Ag*nP*'s.

4. Discussion

Despite the fact that CS/Ag*nP*'s composite exhibited well-defined properties of a percolation system, the most important question is why investigated films have relatively low conductivity, about $5 \cdot 10^{-8}$ S/cm in a film with 17% of Ag*nP*'s? It is important to note that the same low conductivity behavior has been reported in the literature for other Ag*nP*'s/polymer nanocomposites. In [17], it has been reported on that the silver-nitrate-doped chitosan acetate films exhibit an increase of the conductivity to the maximum level up to $2.5 \cdot 10^{-5}$ S/cm. In the poly(vinylidene fluoride)-Ag*nP* system, there was no observation of the percolation effect in the nanocomposite when Ag loading range was within 20% of the Ag*nP*'s, and the ac conductivity at a frequency of 40 Hz was about 10^{-8} S/cm [18]. In the nanocomposites made of epoxy resin filled with 70-nm-sized silver particles, a very low percolation threshold is obtained (1% of Ag*nP*'s), but the dc conductivity in the material with 15% of nanoparticles was about $2 \cdot 10^{-9}$ S/cm [19].

The same relatively low conductivity after the percolation threshold has been observed in polymer/carbon nanotubes composites [20,21]. The explanation of this effect is based upon the existence a thin polymer layer that coexists between carbon nanotubes by using a model which allows calculating the contact resistance between individual carbon nanotubes embedded in a polymer matrix. The contact resistance between silver nanoparticles in a film with 17% of Ag*nP*'s based on this model was estimated to be about $3 \cdot 10^{8}$ Ohm. This value is sufficiently higher than that reported in the literature for polymer/carbon nanotubes (for different polymer matrices, R_c lies in the range 10^{3}–10^{7} Ohm [21]). Results obtained for the investigated CS/Ag*nP*'s composite allow us to explain the low conductivity after the percolation threshold by the presence of a thin polymer layer that coexists between silver nanoparicles. An indirect confirmation of this hypothesis can be obtained from the Fourier

Transformed Infrared (FTIR) spectroscopy analysis which shows that the silver nanoparticles have a strong interaction with OH, NH_2, $CO \cdot NH_2$, and C-O-C groups of the chitosan matrix [6].

Another important observation is the nature of relaxation processes observed in all CS/Ag*nP*'s composites. For various polysaccharide materials, it was found that the activation energies of the dc conductivity and the dielectric relaxations were nearly equal (85–110 kJ/mol) for all substances [22]. This relaxation process is related to the σ-relaxation. The same relaxation process has been observed also in CS/Ag*nP*'s with an activation energy of about 80–86 kJ/mol [6]. Two models in the literature have been discussed for the interpretation of this relaxation process: the first one assumes a local diffusion process of hydrogen ions between high potential barriers in these disordered systems, and the second one considers a conducting pathway through a badly conducting environment in the material [22]. In CS/Ag*nP*'s composite, the σ-relaxation shifts to lower temperatures with increase in the Ag*nP*'s content [6]. This effect can be related to an increase of the amount of Ag^+ ions, which effectively increases the conductivity of CTS/Ag*nP*'s films and points to confirming the hypothesis proposed in [22] that states that the ion hopping in an amorphous solid can lead to a relaxation process.

5. Conclusions

The analysis of the dc conductivity in dry CTS/Ag*nP*'s samples has shown that this composite demonstrates a percolation threshold at the Ag*nP*'s volume fraction of about 2%. Above the percolation threshold, the dc conductivity shows a non-linear behavior with the critical exponent $t = 1.32$, which corresponds to a two-dimensional percolation system. Below the percolation threshold, the temperature dependence of the dc conductivity in the range 2–70°C exhibits the 2-D hopping conductivity according to the variable range hopping model. Above the percolation threshold, the relatively low conductivity values have been attributed to a thin polymer layer which intervenes between silver nanoparicles.

For samples with Ag*nP*'s above 2% in the temperature range 2–180°C and for samples below 2% of Ag*nP*'s in the temperature range 70–180°C, both the conductivity and relaxation times obtained from electrical modulus measurements demonstrate the Arrhenius-type behavior with activation energies between 79 and 86 kJ/mol. This Arrhenius process is associated with the migration property of movable hydrogen ions and the σ-process which corresponds to the formation of dipolar structures. This is a typical behavior for other polysaccharides. The values of activation energy of the σ-process obtained from the electrical modulus presentation correlate well with activation energies calculated from dc conductivity measurements and obtained from fitting the complex permittivity using the Havriliak–Negami model.

Acknowledgment

This work was partially supported by CONACYT of Mexico. The authors are grateful to J. A. Muñoz-Salas for the technical assistance in electrical measurements.

References

[1] Wei, D., Sun, W., Qian, W., Ye, Y., & Mac, X. (2009). *Carbohydrate Research*, *344*, 2375.
[2] Sanvicens, N., Pastells, C., Pascual, N., & Marco, M.-Pilar. (2009). *Trends in Analytical Chemistry*, *25*, 1243.
[3] Wan, Y., Creber, K. A. M., Peppley, B., & Bui, V. T. (2003). *Polymer*, *44*, 1057.
[4] Rhim, J. W., Hong, S. I., Park, H. M., & Ng, P. K. W. (2006). *J. Agric. Food Chem.*, *54*, 5814.
[5] González-Campos, J. B., Prokhorov, E., Luna-Bárcenas, G., Fonseca-García, A., & Sanchez, I. C. (2009). *J. Polym. Sci. B*, *47*, 2259.
[6] González-Campos, J. B., Prokhorov, E., Luna-Bárcenas, J. G., & Mendoza Duarte, M. E. (2010). *J. Polym. Sci. B*, *48*, 739.
[7] Heilmann, A. (2003). *Polymer Films with Embedded Metal Nanoparticles*, Springer: Berlin.
[8] Fraysse, J., & Planes, J. (2000). *Phys. Stat. Sol. (b)*, *218*, 273.
[9] Kirkpatrick, S. (1973). *Rev. Mod. Phys.*, *45*, 574.
[10] Stauffer, D., & Aharony, A. (1994). *Introduction to Percolation Theory*, Taylor & Francis: London.
[11] Wu, J., & McLachlan, D. S. (1998). *Phys. Rev.*, *58*, 14880.
[12] Capaccioli, S., Lucchesi, M., Rolla, P. A., & Ruggeri, G. (1998). *J. Phys.: Condens. Matter.*, *10*, 5595.
[13] Mott, N. F. (1990). *Metal–Insulator Transitions*, Taylor & Francis: London.
[14] Psarras, G. C. (2006). *Composites: Part A*, *37*, 1545.
[15] Köhler, M., Lunkenheimer, P., & Loidl, A. (2008). *Eur. Phys. J. E*, *27*, 115.
[16] Tsangaris, G. M., Psarras, G. C., & Kouloumbi, N. (1998). *J. Mat. Sci.*, *33*, 2027.
[17] Morni, N. M., Mohamed, N. S., & Arof, A. K. (1997). *Mat. Sci. & Engin.*, *B45*, 140.
[18] Huang, X., Jiang, P., & Xie, L. (2009). *Appl. Phys. Lett.*, *95*, 242901.
[19] Gonon, P., & Boudefel, A. (2006). *J. Appl. Phys.*, 024308.
[20] Logakis, E., Pandis, C., Peoglos, V., Pissis, P., Pionteck, J., Potschke, P., Micusık, M., & Omastova, M. (2009). *Polymer*, *50*, 5103.
[21] Kovacs, J. Z., Velagala, B. S., Schulte, K., & Bauhofer, W. (2007). *Comp. Sci. & Tech.*, *67*, 922.
[22] Einfeldt, J., Meibner, D., & Kwasniewski, A. (2003). *J. Non-Cryst. Solids*, *320*, 40.